3D Reconstruction of Underwater Shipwrecks: Structure from Motion and 3D Gaussian Splatting for the Melania Wreck

Authors: Dario Billi 1, Valeria Croce 2, Andrea Piemonte 1, Gabriella Caroti 1
1 Department of Civil and Industrial Engineering, ASTRO Laboratory, University of Pisa, L.go Lucio Lazzarino, 56122 Pisa, Italy; dario.billi@phd.unipi.it; andrea.piemonte@ing.unipi.it, gabriella.caroti@ing.unipi.it
2 LISPEN EA7515, Arts et Métiers Institute of Technology, 2 Cours des Arts et Métiers, 13617 Aix-en-Provence, France; valeria.croce@ensam.eu

Introduction

Documenting **underwater archaeological sites is challenging due to light absorption, turbidity, and backscatter, caustics ect.**

Traditional methods like Structure-from-Motion (SfM) often suffer under these conditions specially for color rendering.

Objective: Integrate traditional photogrammetric methods (focused on metric accuracy) with Gaussian Splatting techniques (focused on realistic, real-time rendering) of existing datasets.

Method:

- **Use a shared set of camera alignment parameters for both the pipelines to ensure consistency between metric and visual outputs.**

Benefits:

- Uses the **same input parameters.**
- Combines **quantitative precision** with **real-time, high-fidelity visualization**.
- **Improves classification and recognition** of flora and fauna, thanks to enhanced visual rendering.
- **Supports marine biologists** and **archeologists** in **documenting ecological features** more effectively, even in visually degraded environments.

Case Study: The Melania Shipwreck
Located off the coast of Vada, Livorno, Italy.

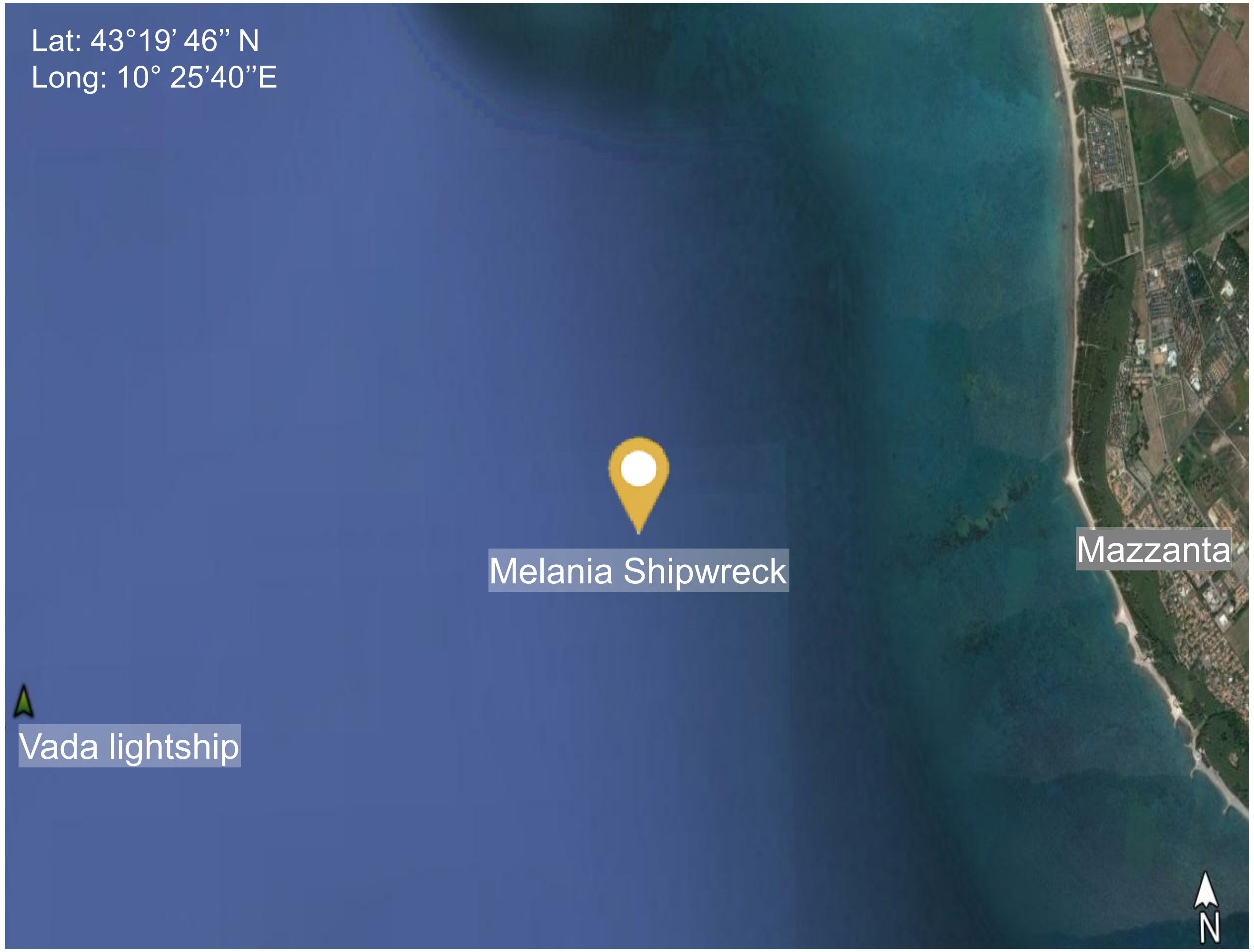

Location of the wreck of the cargo ship Melania from Google Earth

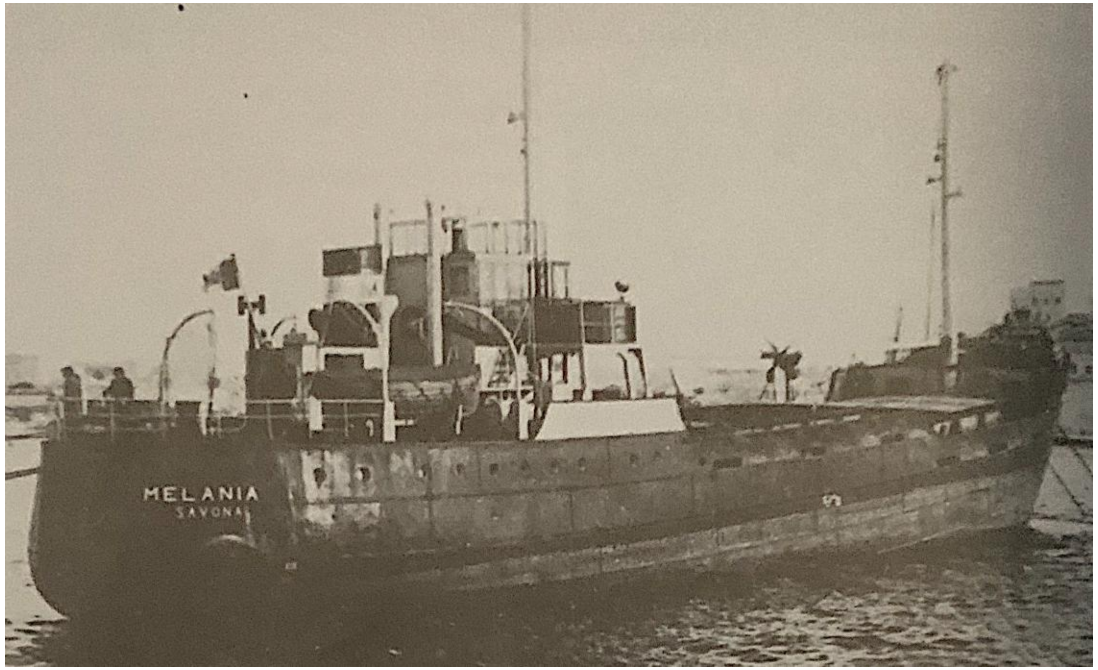

Distance from shore: 1.2 miles
Depth: 7–12 meters
Seabed: rocky platform with sandy areas, largely covered by **Posidonia oceanica** meadows

Survey conducted by *Sub-IA* team.
Photographic data collected by divers.

Dataset

The dataset, provided by *Sub-IA*, was **captured using GoPro cameras mounted on divers**. Several **underwater video sequences** were **recorded**, in order to extract **2649 high-resolution frames (4000 × 3000 px, 300 dpi). Color correction** was **performed in Adobe Lightroom**, **including white balance adjustment** using the gray patch **and RGB channel calibration.** The correction, applied uniformly across the entire dataset, is essential to compensate for spectral attenuation, particularly the loss of red tones at greater depths.

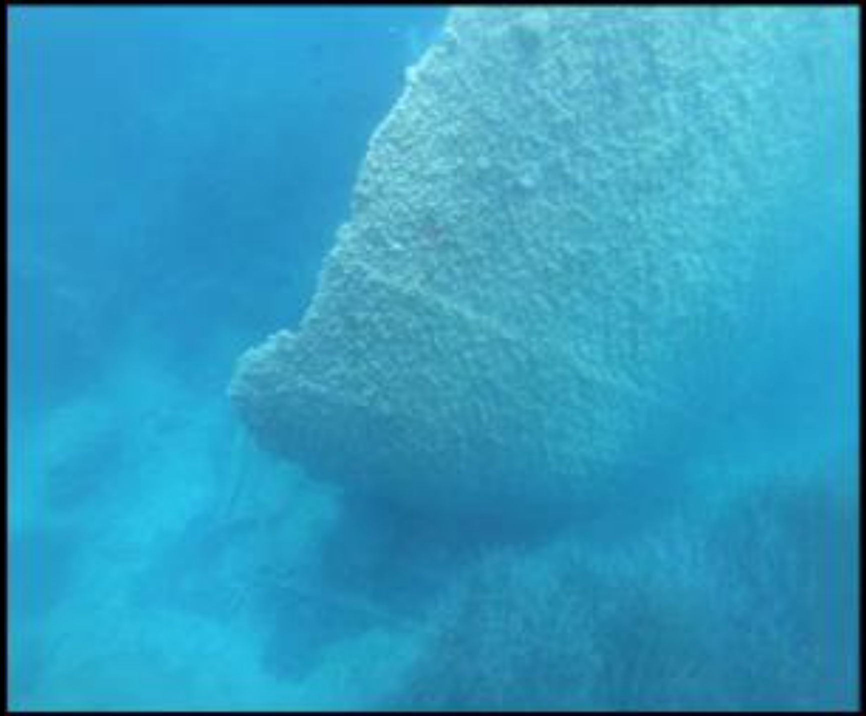

Overview of the proposed methodology

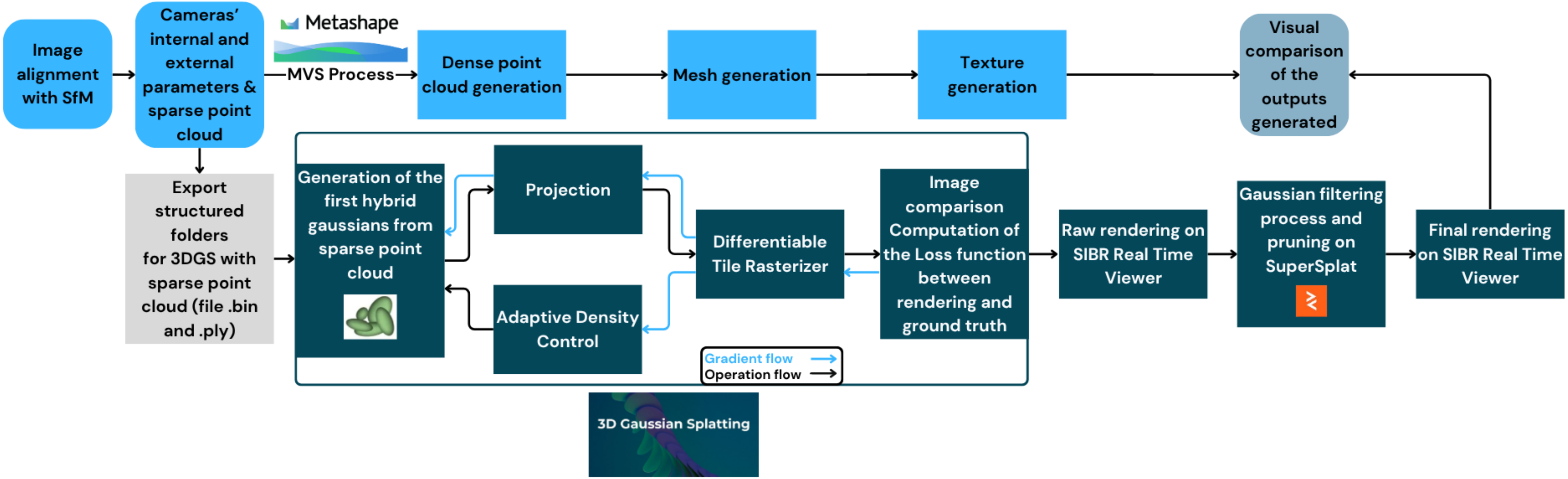

Both **SfM and 3DGS pipelines start from** a **shared sparse point cloud**, generated from the image alignment.

Methodology: Common input

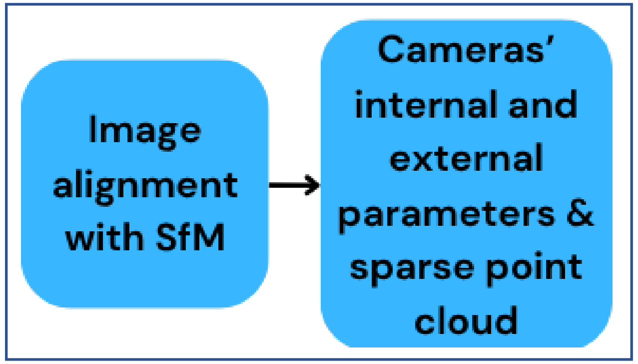

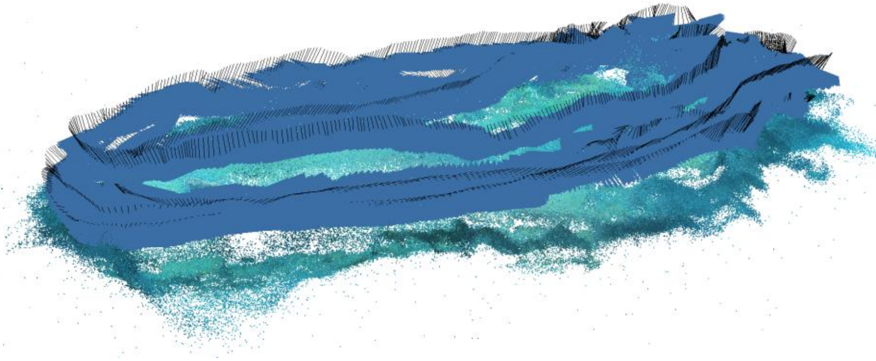

Methodology – Shared Input for SfM and 3DGS

•The process begins with the generation of a **sparse point cloud** from **color-corrected images**.
•This initial step is essential for estimating both the **internal and external parameters** of the cameras.

•Typically, this is done using **COLMAP**, a well-known open-source tool for Structure-from-Motion (SfM).
•**Issue encountered**: COLMAP failed to properly align all images, leading to **incomplete reconstructions** and **inaccurate camera parameters**.

•**Adopted solution**: a **proprietary SfM workflow using Agisoft Metashape** was employed to ensure correct image alignment.

Alignment settings	
Accuracy	High
Limit key points	0
Limit tie points	0
Generic preselection	No
Reference preselection	No
Adaptive camera model fitting	No
Exclude stationary tie points	Yes
Guided image matching	No

Table 1. Common alignment parameters

Methodology: Structure from Motion (SfM)
Multi-view photogrammetry pipeline

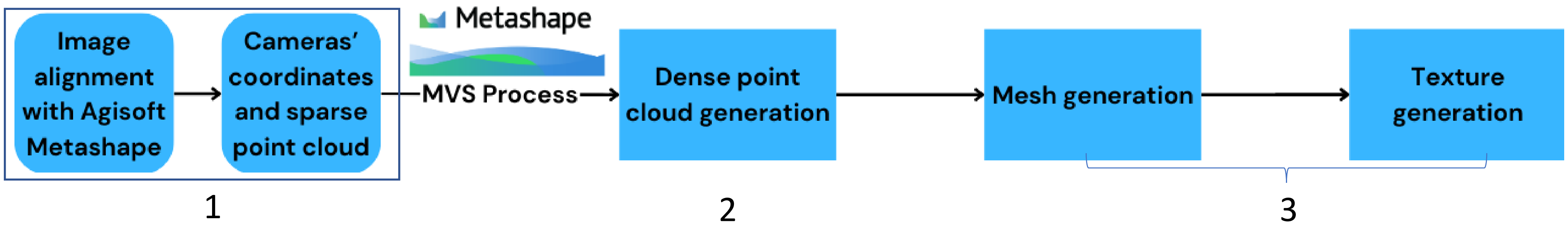

Feature matching
Sparse & dense point cloud generation
Mesh creation and texturing

Mesh settings	
Source data	Depth Maps
Surface type	Arbitrary
Quality	High
Face count	High
Interpolation	Enabled
Depth filtering	Mild

Table 2. Agisoft Metashape parameters to generate mesh model

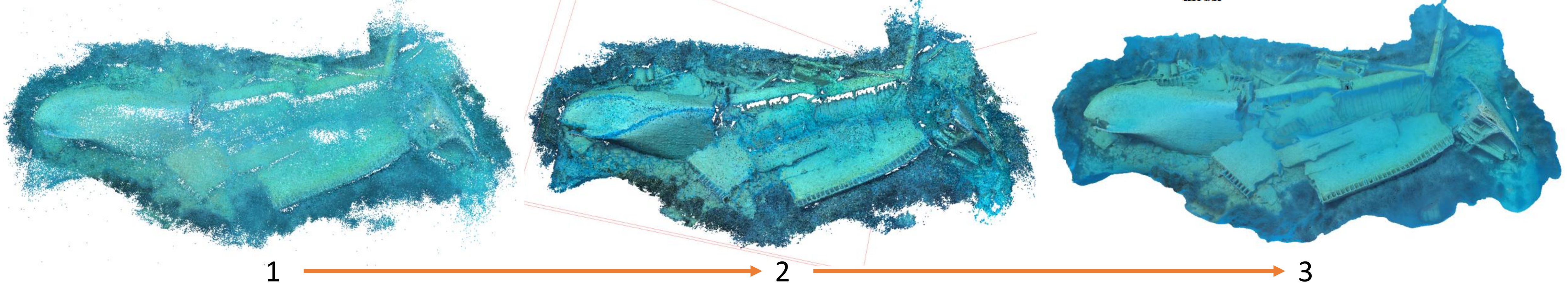

Methodology: 3D Gaussian Splatting (3DGS) Technique for photorealistic 3D rendering pipeline

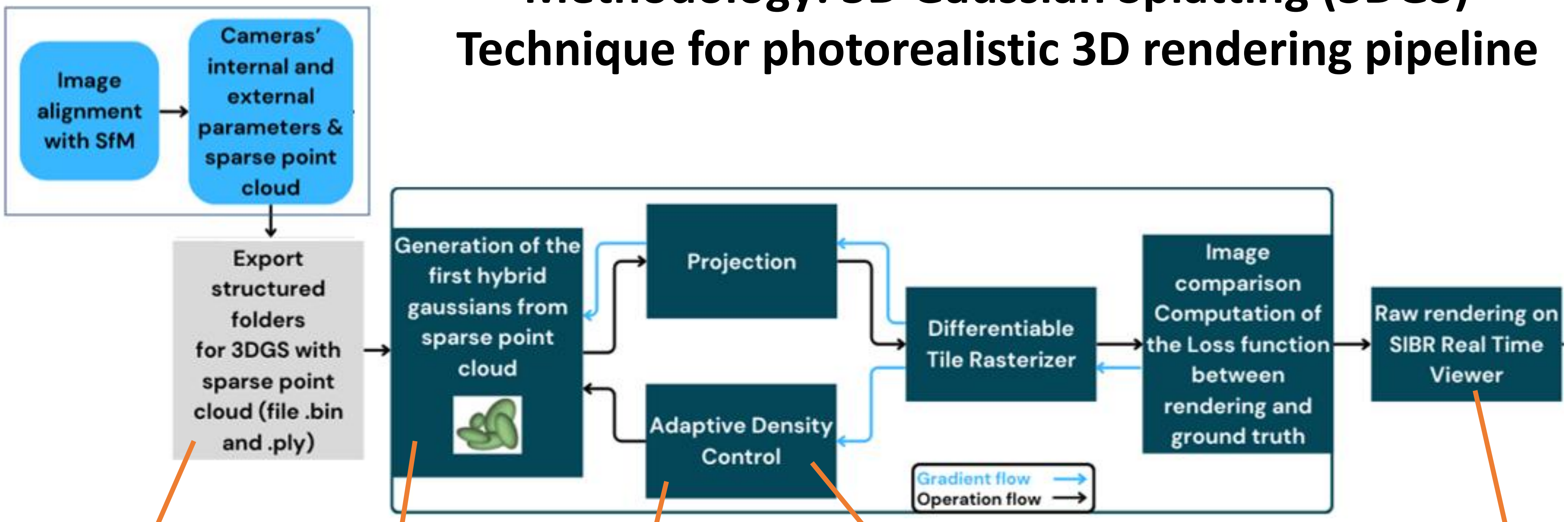

NOTES:
3DGS was **run via Anaconda prompt:**
Using all default settings (30000 iterations) except for **image resolution reduce to 1/8** due to large size dataset.

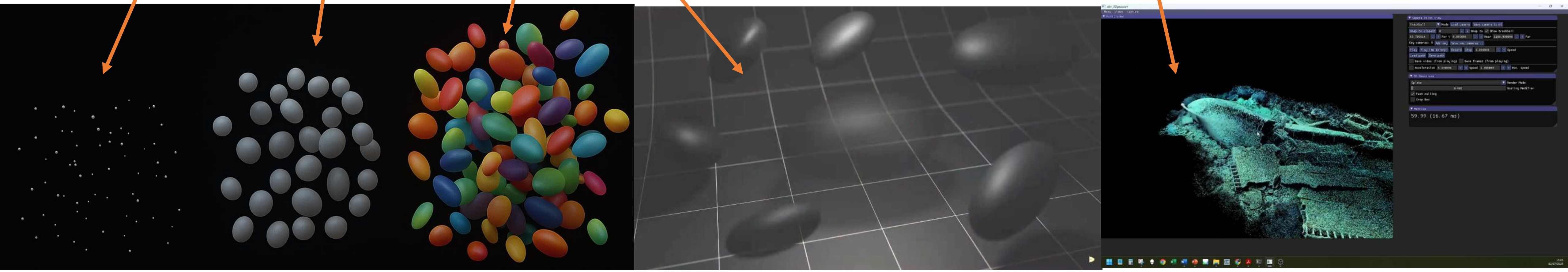

1) **Initialization:** Points are converted into 3D gaussians (starts as spheres). That contains it owns values **x, y, z, Σ, σ(α), SH**

2) **Projection and Rasterization:** Projection **of 3D** gaussians **into 2D** gaussians **parallel to each frame image** (splatting) **creating rendered images**, thanks to the rasterizer.

3) **Comparison between resulted** images and **original** images (ground truth), **computing a loss function to adjust the gaussians values (x, y, z, Σ, σ(α), SH)**.

4) **Adaptive Density Control:** automated densification and pruning of the 3D Gaussians that are too transparent.

Iterations from point 1) to 4) until the rasterized images are closed to the original images.

Methodology: 3D Gaussian Splatting (3DGS)
Technique for photorealistic 3D rendering pipeline

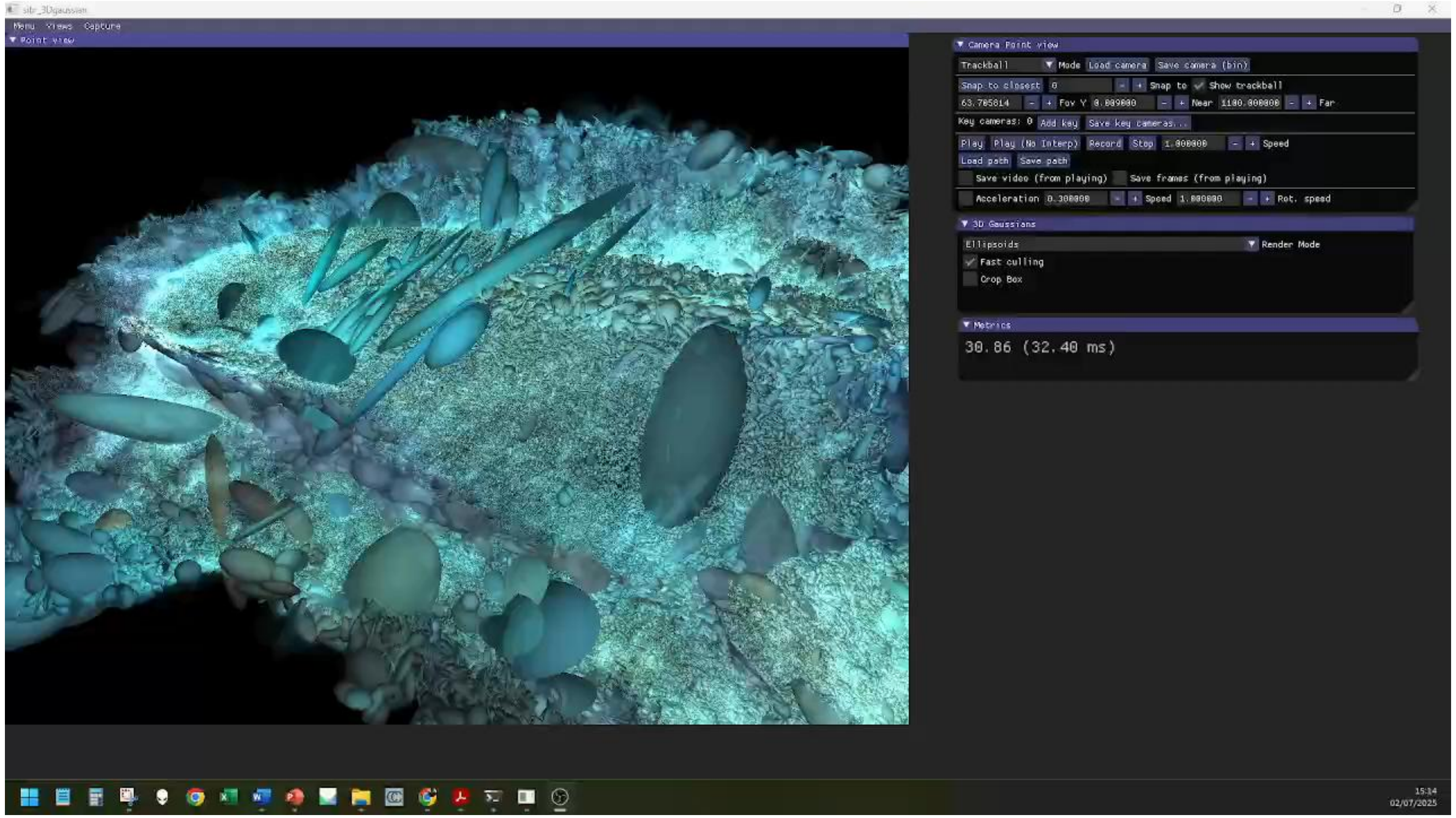

The automatic pruning of superfluous ellipsoids provided by the 3DGS code is often insufficient, making manual intervention necessary.
To this end, SuperSplat an open-source platform based on the PlayCanvas engine **was used to inspect and selectively edit splats directly within a 3D environment.**
Thanks to its support for the PLY format and an intuitive interface, it enabled precise editing (selection, translation, deletion) without the need for local installations, making it an ideal tool for final cleanup and preparation for visualization.

Results: Visual comparison of the outputs generated

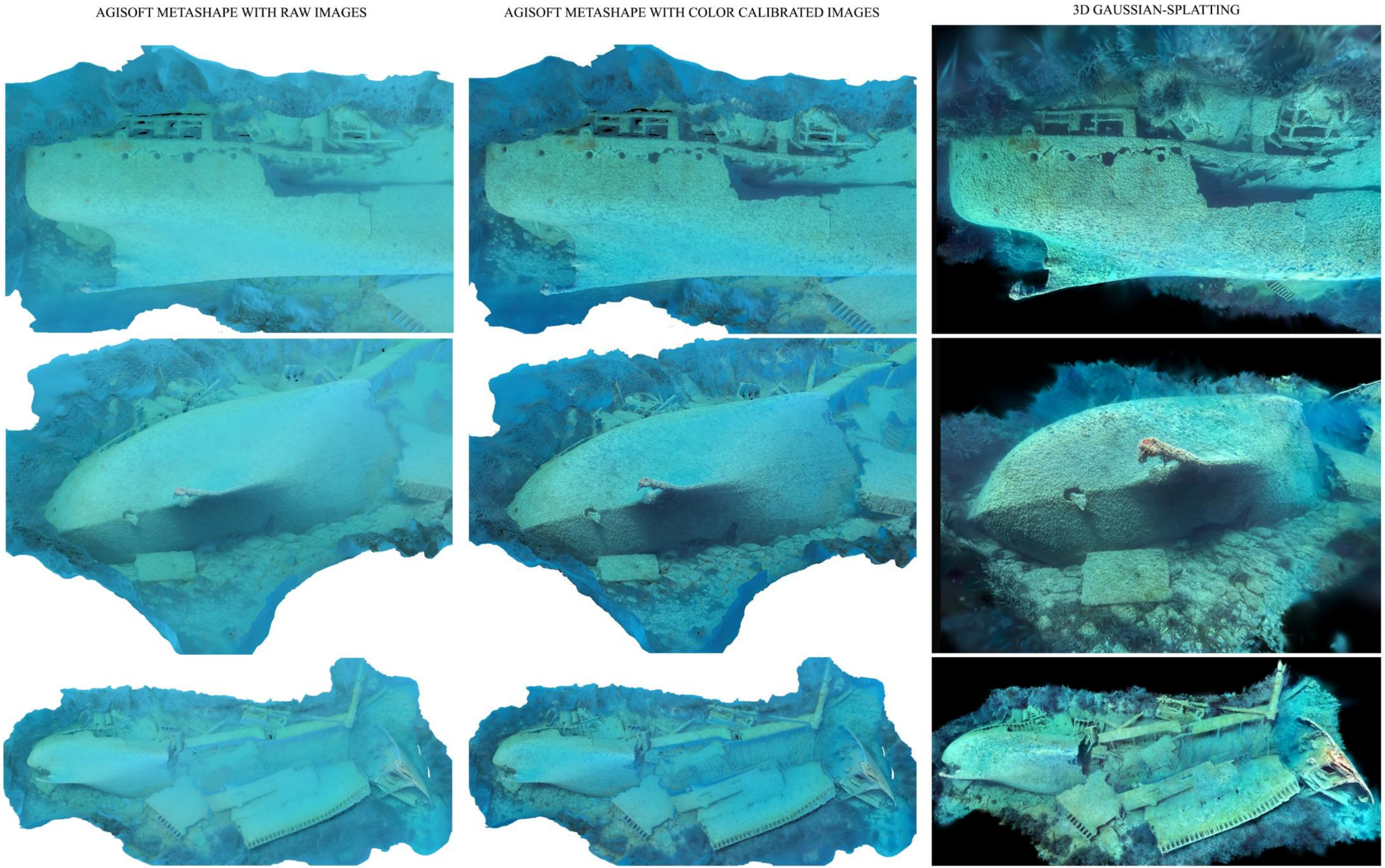

Results: Visual comparison of the outputs generated

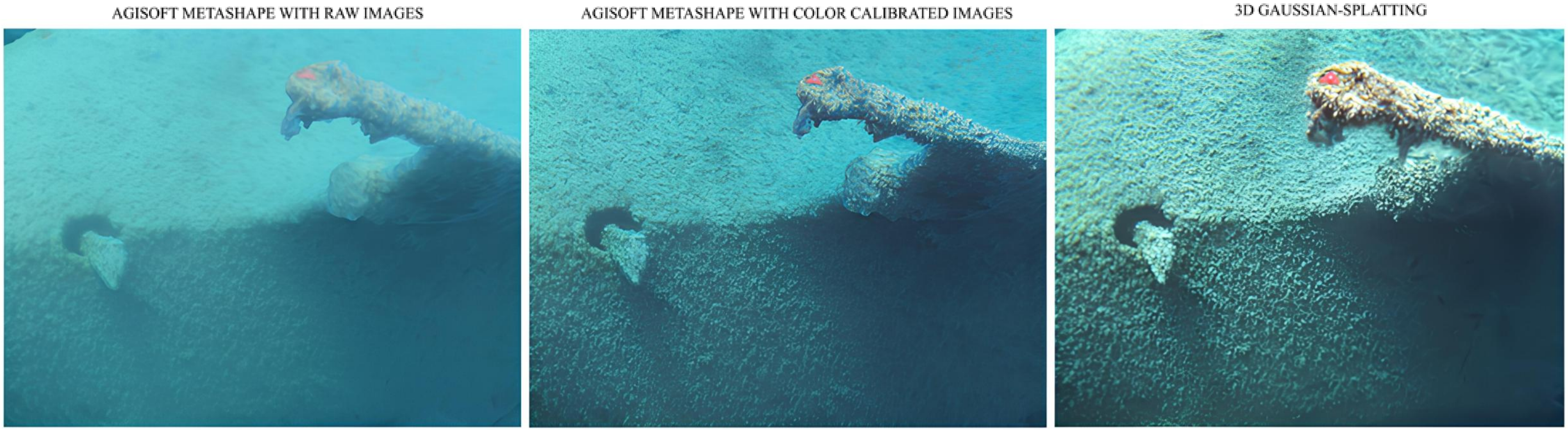

- **Left Image** (**without color correction using SfM**): The colors are rather distorted towards dark blue. There is a lack of saturation and chromatic variety. The loss of color is evident, especially warm tones like red and orange.

- **Central Image** (**with color correction using SfM**): The colors are more varied and closer to what would be expected above water. There is an improvement in saturation and chromatic variety. However, the colors might not be entirely natural or accurate, indicating that the color correction is not perfect.

- **Right Image** (with color correction using 3DGS): The colors appear the most natural and close to what would be expected above water. **There is good saturation and chromatic variety.** The warm and cool tones are balanced in a realistic way, indicating a more accurate color correction.

The 3DGS model produces visually more vibrant and perceptually engaging imagery, particularly in areas most affected by depth-induced light attenuation.

Results: Rendering metrics for 3DGS

Metric	Range	Interpolation
SSIM	> 0.90	Excellent structural similarity
	0.85 – 0.90	High quality
	0.80 – 0.85	Good quality
	<0.80	Noticeable structural degradation
PSNR	> 27	Very high visual fidelity
	23 – 27	High quality
	20 – 23	Medium/acceptable quality
	< 20	Perceptible degradation
LPIPS	< 0.10	Excellent perceptual similarity
	0.10 – 0.15	High perceptual quality
	0.15 – 0.20	Medium quality
	> 0.20	Low perceptual fidelity/perceptible error

Table 3. Metric quality thresholds for underwater scenes estimated using as reference, WaterSplatting (Li et al., 2024) and SeaSplat (Yang et al., 2024)

METRICS	
WITHOUT SUPERSPLAT EDITING	
SSIM	0.79
PSNR	25.24
LPIPS	0.29

Table 4. Rendering metrics values

- **PSNR (Peak Signal-to-Noise Ratio):** measures pixel-by-pixel difference between two images. Sensitive to noise, doesn't reflect human perception well.
- **SSIM (Structural Similarity Index):** evaluates structural similarity (luminance, contrast, structure). Closer to human visual perception than PSNR.
- **LPIPS (Learned Perceptual Image Patch Similarity):** uses neural networks to assess perceptual similarity. It's the most aligned with human perception, especially for complex images.

Results: Time processing

The image alignment phase, common to both methods, **is the most time-consuming step** as it involves **calculating internal and external camera parameters** using **Structure-from-Motion (SfM)** in **Agisoft Metashape**.

After this phase:

The generation of the solid and textured model via Metashape **takes twice (78min)** as long **compared to the creation of the synthetic model viewable** in real time via **3D Gaussian Splatting (40min).**

3D Gaussian Splatting, is based on synthetic rendering, which is lighter and faster suitable for visualization but not for metric accuracy.

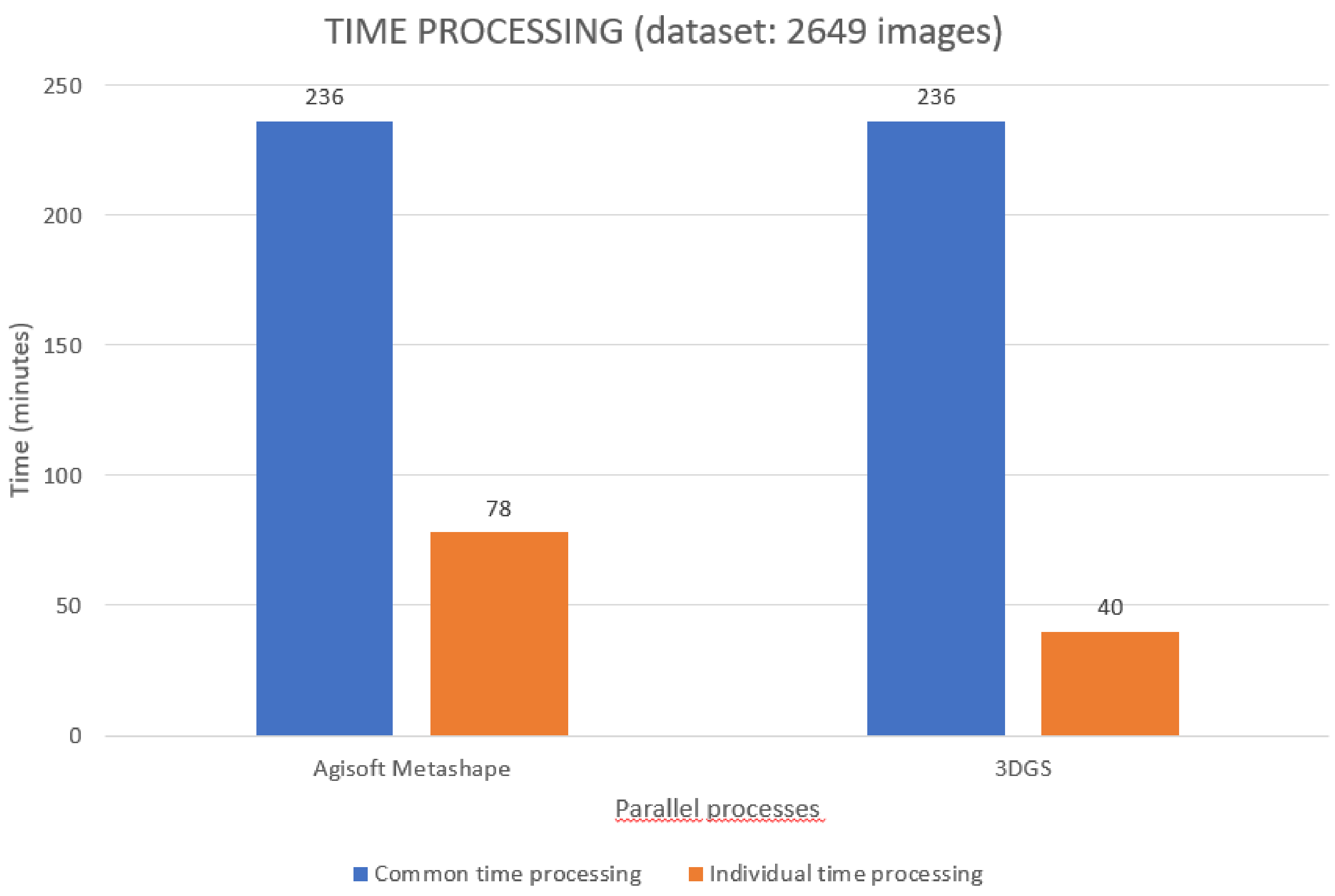

Conclusions

Advantages of the integrated approach

The generation of two complementary types of models using common photogrammetric parameters :

Geometric model:

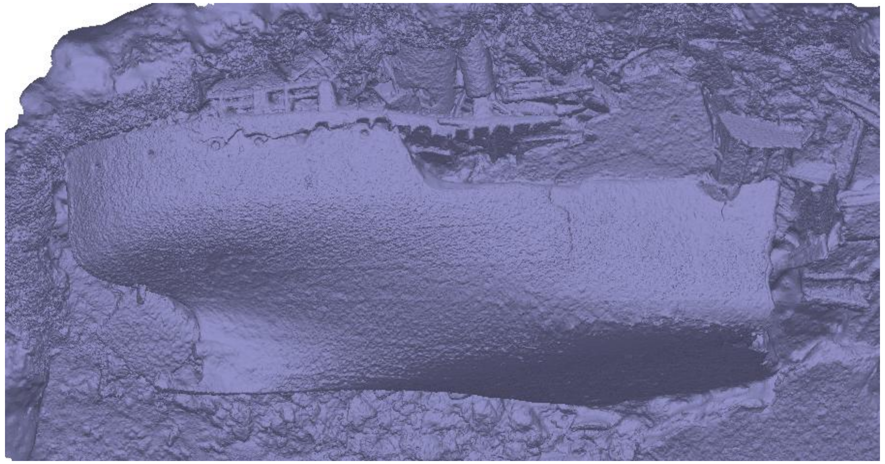

- Suitable for **metric and scientific studies**.
- Essential for the **survey of submerged cultural heritage (archeologists)**.

Real time rendering model (3DGS):

- Ideal for **scientific communication and outreach**.
- Useful for **ecological and environmental analysis** of **marine settlements (biologists)**.
- **Based on synthetic rendering,** which is **lighter and faster** suitable **for visualization.**
- **Improves color rendering,** particularly of **reds and warm tones**, increasing the ability to **more easily identify flora and fauna settled on the wrecks.**

Future Works

- **Exploration of specialized renderers** like **SeaSplat**, **WaterSplatting**, (ect) **which are still underused** or **partially unavailable in the open-source community**.

- Gradual replacement of proprietary software (e.g., **Agisoft Metashape**) with open-source alternatives like **Deep Image Matching or Reality Capture**.

- The **extension of the pipeline** to **more complex or dynamic new underwater scenarios.**

- **Include generating mesh models from Gaussian Splatting**, that **we already tested in our research on terrestrial critical datasets** (e.g., using plug-in from native code as **SuGaR**, **2D Gaussian Splatting**), promising **efficient geometry and high visual quality.**

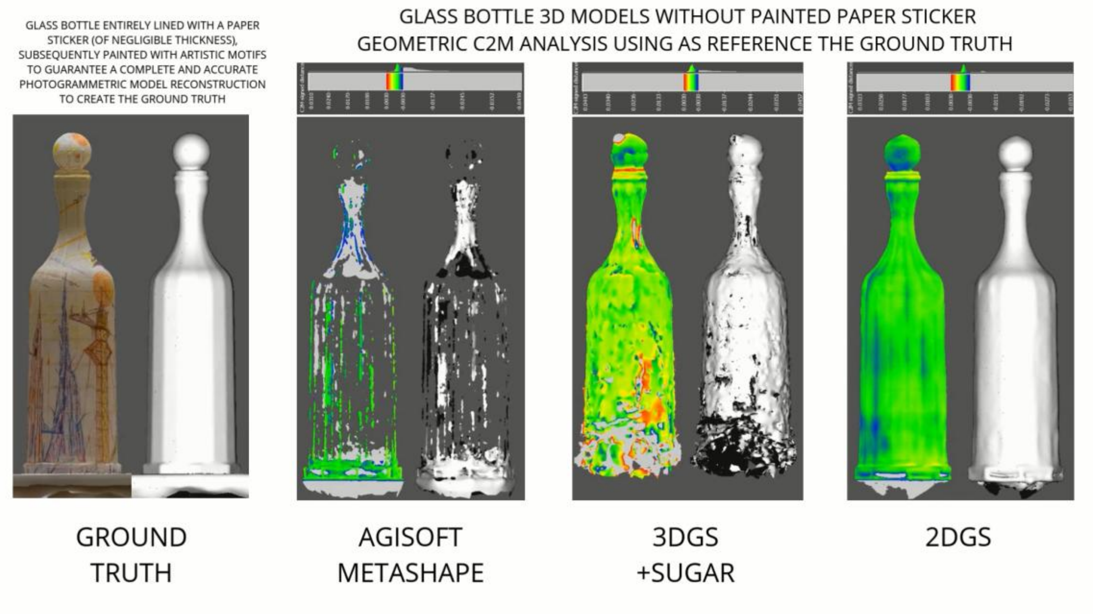

References

Adams, D., Helmholz, P., McMeekin, D., & Woods, A. (2024). Improving Underwater Photogrammetric 3D Reconstruction Processing of Shipwreck Sites. *ISPRS Annals of the Photogrammetry, Remote Sensing and Spatial Information Sciences*, X-4-2024, 7–14. DOI: 10.5194/isprs-annals-X-4-2024-7-2024

Calantropio, A., Chiabrando, F., Seymour, B., Kovacs, E., Lo, E., Rissolo, D., 2020. Image Pre-Processing Strategies for Enhancing Photogrammetric 3D Reconstruction of Underwater Shipwreck Datasets. ISPRS Arch. Photogramm. Remote Sens. Spatial Inf. Sci., XLIII-B2-2020, 941–948. https://doi.org/10.5194/isprs-archives-XLIII-B2-2020-941-2020.

Croce, V., Caroti, G., De Luca, L., Piemonte, A., Véron, P., 2023. Neural Radiance Fields (NeRF): Review and Potential Applications to Digital Cultural Heritage. ISPRS Arch. Photogramm. Remote Sens. Spatial Inf. Sci., XLVIII-M-2-2023, 453–460. https://doi.org/10.5194/isprs-archives-XLVIII-M-2-2023-453-2023.

Doležal, M., Vlachos, M., Secci, M., Demesticha, S., Skarlatos, D., & Liarokapis, F. (2019). Understanding Underwater Photogrammetry for Maritime Archaeology Through Immersive Virtual Reality. *International Archives of the Photogrammetry, Remote Sensing and Spatial Information Sciences*, XLII-2/W10, 85–91. DOI: 10.5194/isprs-archives-XLII-2-W10-85-2019

Drap, P., Merad, D., Mahiddine, A., Boi, J.M., Chemisky, B., Long, L., Seinturier, J., 2015. Underwater Photogrammetry and Object Modeling: A Case Study of Xlendi Wreck in Malta. Sensors, 15(12), 30351–30384. https://doi.org/10.3390/s151229802.

Du, Y., Zhang, Z., Zhang, P., Sun, F., Lv, X., 2024. UDR-GS: Enhancing Underwater Dynamic Scene Reconstruction with Depth Regularization. Symmetry, 16(8), 1010. https://doi.org/10.3390/sym16081010.

Fan, X., Wang, X., Ni, H., Yuanxue, X., & Shi, P. (2025). Water-Adapted 3D Gaussian Splatting for Precise Underwater Scene Reconstruction. *Remote Sensing*.

Iandola, F.N., Han, S., Moskewicz, M.W., Ashraf, K., Dally, W.J., Keutzer, K., 2016. SqueezeNet: AlexNet-Level Accuracy with 50x Fewer Parameters and <0.5MB Model Size. arXiv preprint arXiv:1602.07360.

Kerbl, B., Kopanas, G., Leimkühler, T., Drettakis, G., 2023. 3D Gaussian Splatting for Real-Time Radiance Field Rendering. ACM Trans. Graph., 42(4), 1–14. https://doi.org/10.1145/3592433.

Krizhevsky, A., Sutskever, I., Hinton, G.E., 2012. ImageNet Classification with Deep Convolutional Neural Networks. Adv. Neural Inf. Process. Syst. (NIPS 2012), 25, 1097–1105.

Li, H., Song, W., Xu, T., Elsig, A., Kulhanek, J., 2024. WaterSplatting: Fast Underwater 3D Scene Reconstruction Using Gaussian Splatting. arXiv:2408.08206. https://arxiv.org/abs/2408.08206.

Mildenhall, B., Srinivasan, P.P., Tancik, M., Barron, J.T., Ramamoorthi, R., Ng, R., 2020. NeRF: Representing Scenes as Neural Radiance Fields for View Synthesis. ECCV 2020. https://arxiv.org/abs/2003.08934.

Mualem, N., Amoyal, R., Freifeld, O., Akkaynak, D., 2024. Gaussian Splashing: Direct Volumetric Rendering Underwater. arXiv:2411.19588. https://arxiv.org/abs/2411.19588.

Nocerino, E., Menna, F., Remondino, F., Toschi, I., & Fassi, F. (2020). Coral Reef Monitoring by Scuba Divers Using Underwater Photogrammetry and Geodetic Surveying. *Remote Sensing*, 12(18), 3036. DOI: 10.3390/rs12183036

Simonyan, K., Zisserman, A., 2014. Very Deep Convolutional Networks for Large-Scale Image Recognition. arXiv preprint arXiv:1409.1556.

Song, Y., She, M., & Köser, K. (2023). Advanced Underwater Image Restoration in Complex Illumination Conditions. *arXiv preprint arXiv:2309.02217*. https://arxiv.org/abs/2309.02217

Vlachos, M., & Skarlatos, D. (2021). An Extensive Literature Review on Underwater Image Colour Correction. *Sensors*, 21(17), 5690. DOI: 10.3390/s21175690

Wang, H., Anantrasirichai, N., Zhang, F., Bull, D., 2024. UW-GS: Distractor-Aware 3D Gaussian Splatting for Enhanced Underwater Scene Reconstruction. arXiv:2410.01517. https://arxiv.org/abs/2410.01517.

Wang, Z., Bovik, A.C., Sheikh, H.R., Simoncelli, E.P., 2004. Image Quality Assessment: From Error Visibility to Structural Similarity. IEEE Trans. Image Process., 13(4), 600–612.

Yang, D., Leonard, J.J., Girdhar, Y., 2024. SeaSplat: Representing Underwater Scenes with 3D Gaussian Splatting and a Physically Grounded Image Formation Model. arXiv:2409.17345. https://arxiv.org/abs/2409.17345.

Zhang, R., Isola, P., Efros, A.A., Shechtman, E., Wang, O., 2018. The Unreasonable Effectiveness of Deep Features as a Perceptual Metric. In: Proc. IEEE Conf. Comput. Vis. Pattern Recognit. (CVPR), Salt Lake City, UT, USA, 586–595.

Zhang, T., Zhi, W., Huang, K., Mangelson, J., Barbalata, C., Johnson-Roberson, M., 2024. RecGS: Removing Water Caustic with Recurrent Gaussian Splatting. arXiv:2412.03435.